Oral Radiol (2009) 25:149–153
DOI 10.1007/s11282-009-0019-8

TECHNICAL REPORT

The effect of voxel size on image reconstruction in cone-beam computed tomography

Hideyuki Tanimoto · Yoshinori Arai

Received: 25 February 2009 / Accepted: 10 May 2009 / Published online: 10 July 2009

Abstract
Objectives This study evaluated the effects of changing the voxel size on the resolution and noise of cone-beam computed tomography (CBCT) reconstruction images.
Methods The voxel sizes used for reconstruction were 160, 80, and 40 μm using prototype software for the Accuitomo F8 (J. Morita, Kyoto, Japan). The resolution was measured using a modulation transfer function (MTF), and CBCT images of a 1-mm-thick, 10-mm-diameter aluminum pipe set slightly inclined from the vertical were taken with a field of view of 8 cm. To measure the noise, a tomographic image of an 8-cm-diameter water phantom was taken and reconstructed at the three voxel sizes. The standard deviation (SD) of the noise was then determined.
Results The MTF at 2 lp/mm was 0.05, 0.12, and 0.12 for voxel sizes of 160, 80, and 40 μm, respectively, and the SD of the noise was 10.0, 13.8, and 17.1% for the same respective voxel sizes.
Conclusions The limit of resolution was determined to be the 80-μm voxel size. When the voxels were smaller, the noise increased.

Keywords Cone-beam computed tomography · Resolution · Noise · Reconstruction

H. Tanimoto (✉) · Y. Arai
Kitasenju Radist Dental Clinic i-VIEW Imaging Center, Koushin Building, 3-59 Senju, Adachi-ku, 120-0034 Tokyo, Japan
e-mail: grht24269@nifty.com

Y. Arai
Nihon University School of Dentistry, Tokyo, Japan

Introduction

In 1997, Arai et al. [1] developed cone-beam computed tomography (CBCT) for the diagnosis of impacted teeth, apical lesions, periodontitis, root fractures, enostosis, and temporomandibular joint disease [2–7]. The imaging area was originally 4 cm in diameter by 3 cm in height, and their machine was characterized by a high resolution and low-radiation dose. The voxel size was 0.125 mm isotropic because the image area was small. Images with this system could discern the periodontal ligament space very clearly [8], and the small radiation field of this machine resulted in a low exposure compared to other CBCT machines [9, 10].

Subsequently, many other types of CBCT were developed [11–15], most of which could image large areas of the maxilla and mandible. Decreasing the noise, pixel size, or slice thickness while the other factors remained constant resulted in an increased patient dose [16]. In these CBCT systems, the voxel sizes used were 0.2–0.4 mm because of computational limitations. If the imaging area measured 8 cm in diameter by 8 cm in height, and a voxel size of 0.125 mm was applied, one would have 640 × 640 × 640 voxels. Similarly, for a voxel size of 0.080 mm, 1,000 × 1,000 × 1,000 voxels would be obtained, which made reconstruction difficult using personal computers.

To solve this problem, the newest Accuitomo F8 (J. Morita, Kyoto, Japan) was developed with a maximum field of view (FOV) of 8 × 8 cm and a zoom reconstruction function. When the raw data are reconstructed, the function decreases the voxel size (zoom), which enlarges the image. To use this function, the region of interest (ROI) on the image is first chosen and then the region is reconstructed with a smaller voxel size.

This study evaluated the resolution and noise when the function is applied with chosen voxel sizes of 40, 80, and 160 μm.

Materials and methods

This study used the zoom reconstruction function of prototype software for the Accuitomo F8. Applying this function changed the original voxel size of 160 μm to 80 or 40 μm (Fig. 1).

Resolution

A 1-mm-thick, 10-mm-diameter aluminum pipe was placed slightly inclined to the vertical (Fig. 2). A CBCT image of the pipe was taken under the following scanning conditions: FOV of 8 cm, at 60 kV and 1 mA, with a focus-to-detector distance of 710 mm, a focus-to-objective distance of 500 mm, and exposure time of 17 s. The CBCT image was constructed with 512 views.

On the CBCT image, an ROI 40 mm in diameter and 40 mm in height was chosen with the pipe at the center of the image in the coronal section. Then, the zoom reconstruction function was applied to the image and the voxel size was changed from 160 μm to 80 or 40 μm. Then, the three resulting images of the pipe were sliced at widths of 160 μm. Consequently, when the voxel size was 40 μm, the voxel direction in the width was four times greater, which meant that the dimensions of a voxel were 40 × 40 × 160 μm. Similarly, when the voxel size was 80 μm, the dimensions of a voxel were 80 × 80 × 160 μm; and the dimensions of a voxel were 160 × 160 × 160 μm when the voxel size was 160 μm.

The line profiles were measured on the three different images obtained using the zoom reconstruction function. Then, the resolution was calculated via the modulation transfer function (MTF) using the edging method [17, 18].

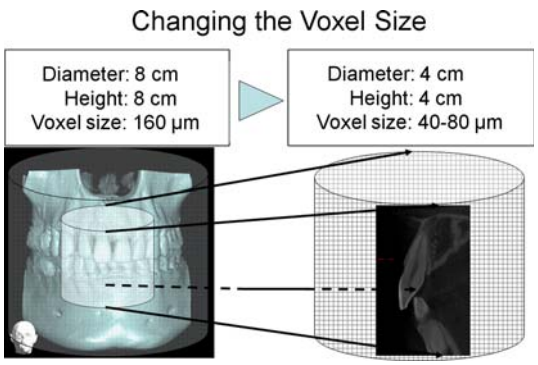

Fig. 1 Changing the voxel size. The zoom reconstruction function changed the voxel size from 160 to 80 or 40 μm

Fig. 2 First step in measuring the MTF. An aluminum pipe was set on the Accuitomo F8 at a slight inclination to the vertical

Noise

A tomographic image of an 8-cm-diameter water phantom was obtained and the image was reconstructed at the three voxel sizes. Then, the standard deviation (SD) of the noise was measured from the three images. The ROI on the images was in the same area and position, which was 4.96 × 4.96 mm at the center of the water phantom.

Visual example

A CBCT image of a phantom of a human dry skull with soft-tissue equivalent material (Type XX; Kyoto Kagaku, Kyoto, Japan) was taken. The scanning conditions were 90 kV and 4 mA, and all the other CBCT settings were the same as described above. The image of the apical root of an upper incisor was reconstructed at the three voxel sizes.

Results

Figure 3 shows CBCT images of the edge of the aluminum pipe taken at each voxel size. The horizontal arrows indicate the main scan direction and the vertical arrows denote the sub-scan direction [7, 8]. A graphic representation of the result is given in Fig. 4. The line profile is indicated for each voxel size. The line profile for 160 μm was gentler than that for 80 and 40 μm. The MTF was calculated from the line profile (Fig. 5) at 2 lp/mm and was 0.05, 0.12, and 0.12 at voxel sizes of 160, 80, and 40 μm, respectively. For all three voxel sizes, the MTF at 3.5 lp/mm was 0.

Figure 6 shows CBCT images of the water phantom taken at each voxel size: the smaller the voxel size was, the greater the noise. The SD values were 10.0, 13.8, and 17.1% at respective voxel sizes of 160, 80, and 40 μm.

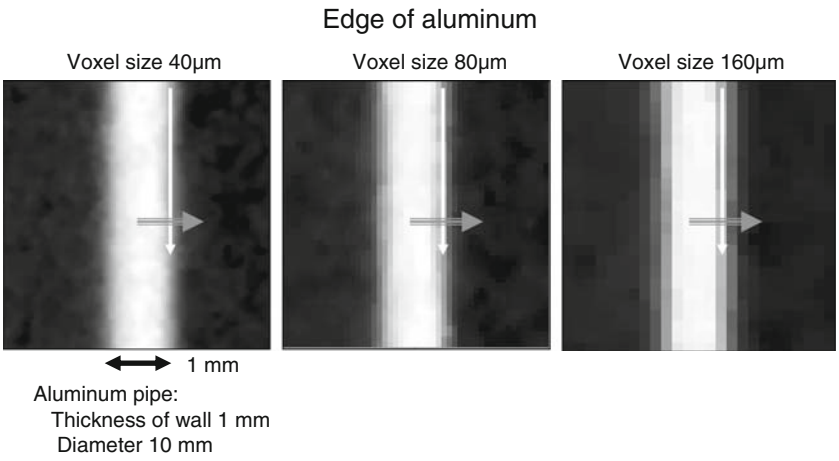

Fig. 3 The edge of the aluminum pipe wall at each voxel size. The pipe images were inclined slightly. The *gray arrow* indicates the main scan and the *white arrow* denotes the sub-scan used for the edge method

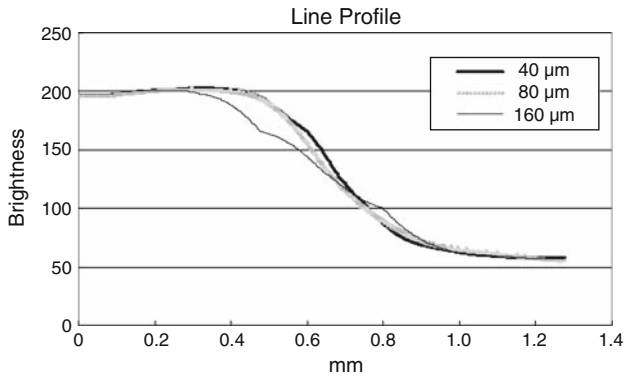

Fig. 4 The line profile of the aluminum pipe wall at each voxel size

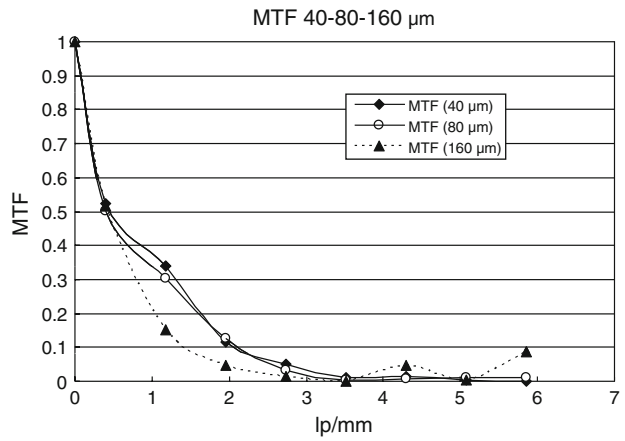

Fig. 5 The MTF at each voxel size. At 2 lp/mm, the results were similar for the 40 and 80 μm voxel sizes, while the values for 160 μm were lower

Visual examples are shown in Fig. 7. The authors evaluated the images subjectively. Specifically, the periodontal ligament space on the palatal side could not be observed clearly at the 160-μm voxel size, while the image with the 40-μm voxel size had the most noise subjectively.

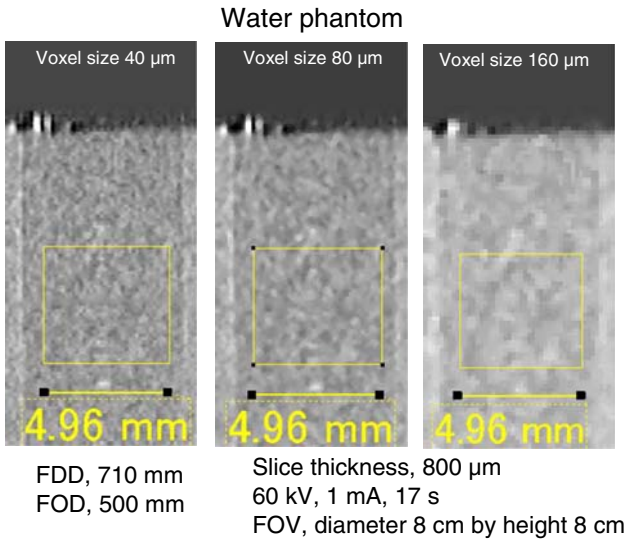

Fig. 6 Tomographic images of a water phantom at each voxel size. The ROI had the same area and was in the same position. The noise increased at smaller voxel sizes

Discussion

Before the newest Accuitomo F8 was developed, a wide FOV required a larger voxel size due to computational limitations, and additional problems were involved. First, the resolution was limited. Even at the smallest voxel size, the resolution could not be increased. This limitation resulted from the focus size of the X-ray tube, the pixel size of the sensor, and the precision of rotation. Second, when the voxel size was small, the noise increased [16, 19]. In such cases, the radiation dose must be increased to reduce the noise, but this is impractical based on the principle of "as low as reasonably achievable" (ALARA) [20].

With the newest Accuitomo F8, the zoom reconstruction function improved the image resolution. On choosing an ROI in the image, only the chosen region is reconstructed with a smaller voxel size. Although the voxel size is small,

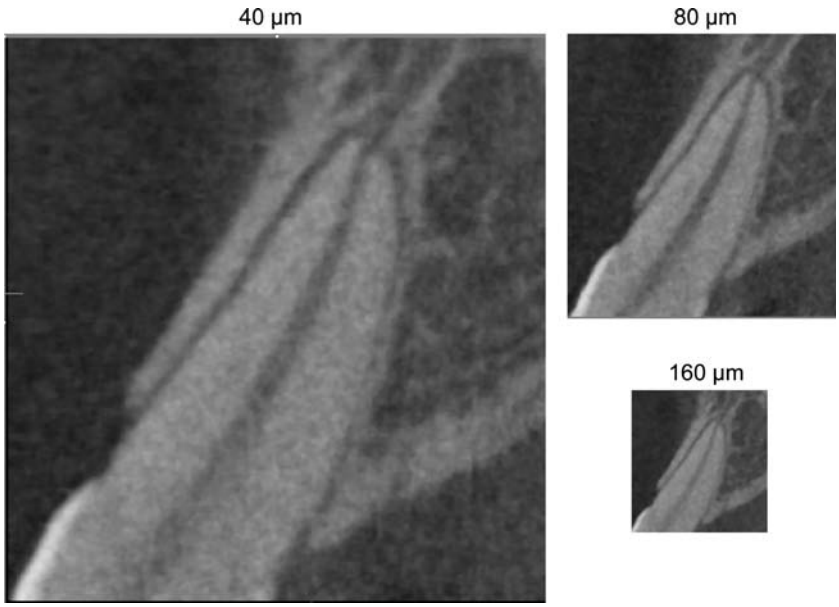

Fig. 7 Human phantom images at each voxel size. The 40-μm voxel size was noisier than the 80-μm size but had slightly better resolution

the image reconstruction time is reduced as only a narrow region is reconstructed, which decreases the computer load. This is thought to be useful in the clinical setting.

The MTF can be calculated in various ways [16]. For example, a very narrow metal wire can be used to measure the fast Fourier transform. In this study, the smallest voxel size was 40 μm, which meant that a metal wire 40 μm in diameter would be required. Therefore, using wire was not practicable. Moreover, a very narrow wire would not produce good contrast, and a high level of noise would result. As an alternative, we used an aluminum pipe and the edge of the pipe was used for the MTF. The wall of the aluminum pipe provided sufficient edge contrast for the measurement.

The resolution was limited when the voxel size was changed [16, 19]. In this study, the MTF in Fig. 5 shows no improvement between voxel sizes of 40 and 80 μm.

The noise is constrained by the number of photons within the voxel unit [16, 21]. The smaller the voxel size is, the fewer photons there are, increasing the noise.

When the pixel size is halved, the noise is $2 \times \sqrt{2}$ [16] because when the pixel size of the sensor is halved, the imaging area is quadrupled and so the width of the X-ray transmission is halved. In contrast, with the zoom reconstruction function in this study, when the voxel size was halved, the noise value was approximately $\sqrt{2}$. This differs from the theoretical value because when the value was calculated, the size of the sensor remained unchanged.

Choosing a small voxel size without changing the radiation dose increases the resolution. There was, however, a limit to the resolution, while there was no limit to the increase in the noise. As a result, with a voxel size of 40 μm, the human phantom image contained a large amount of noise. With a voxel size of 160 μm, the image contained less noise than at 40 μm, but compared to a voxel size of 80 μm, the periodontal ligament space was not obvious. In addition, the resolution was similar at voxel sizes of 40 and 80 μm.

Increasing the radiation dose can reduce the noise at a small voxel size. However, when CBCT is used clinically, we must optimize the resolution, noise, and radiation dose. When a high-resolution image is required, one should choose a voxel size of 80 μm, a limited FOV (e.g., a diameter of 4 cm and a height of 4 cm), and a standard radiation dose. For planning dental implants over a large area, one should choose a voxel size of 160 μm and a low radiation dose to improve the noise in the images.

When the zoom reconstruction function decreases the voxel size, the resolution increases somewhat. Conversely, the smaller the voxel size becomes, the greater the noise will be. To decrease the noise, one has to increase the radiation dose, making the dose a concern. Therefore, the voxel size should not be decreased needlessly.

There is a lower limit to the effect of voxel size on improving the image. With the Accuitomo F8, no improvement in the resolution was observed when the voxel size was $\leq$80 μm.

Acknowledgments We thank J. Morita Corporation, Kyoto, Japan, for supporting this study.

References

1. Arai Y, Tammisalo E, Iwai K, Hashimoto K, Shinoda K. Development of a compact computed tomographic apparatus for dental use. Dentomaxillofac Radiol. 1999;28:245–8.

2. Terakado M, Hashimoto K, Arai Y, Honda M, Sekiwa T, Sato H. Diagnostic imaging with newly developed ortho cubic super-high resolution computed tomography (Ortho-CT). Oral Surg Oral Med Oral Pathol Oral Radiol Endod. 2000;89:509–18.
3. Hashimoto K, Arai Y, Iwai K, Kawashima S, Terakado M. A comparison of a new limited cone beam computed tomography machine for dental use with a multidetector row helical CT machine. Oral Surg Oral Med Oral Pathol Oral Radiol Endod. 2003;95:371–7.
4. Honda K, Arai Y, Kashima M, Takano Y, Sawada K, Ejima K, et al. Evaluation of the usefulness of the limited cone-beam CT (3DX) in the assessment of the thickness of the roof of the glenoid fossa of the temporomandibular joint. Dentomaxillofac Radiol. 2004;33:391–5.
5. Araki M, Hashimoto K, Kawashima S, Matsumoto K, Akiyama Y. Radiographic features of enostosis determined with limited cone-beam computer tomography in comparison with rotational panoramic radiography. Oral Radiol. 2006;22:27–33.
6. Kagawa T, Fukunari F, Shiraishi T, Yamasaki M, Ichihara T, Kihara Y, et al. Development of a simple image designed for small x-ray field CT equipment 3DX. Oral Radiol. 2006;22:47–51.
7. Sakabe J, Kuroki Y, Fujimaki S, Nakajima I, Honda K. Reproducibility and accuracy of measuring unerupted teeth using limited cone beam x-ray CT. Dentomaxillofac Radiol. 2007;36:2–6.
8. Suomalainen AK, Salo A, Robinson S, Peltola JS. The 3DX multi-image micro-CT device in clinical dental practice. Dentomaxillofac Radiol. 2007;36:80–5.
9. Lofthag-Hansen S, Thilander-Klang A, Ekestubbe A, Helmrot E, Gröndahl K. Calculating effective dose on a cone beam computed tomography device: 3D Accuitomo and 3D Accuitomo FPD. Dentomaxillofac Radiol. 2008;37:72–9.
10. Hirsch E, Wolf U, Heinicke F, Silva MAG. Dosimetry of the cone beam computed tomography Veraviewepocs 3D compared with the 3D Accuitomo in different fields of view. Dentomaxillofac Radiol. 2008;37:268–73.
11. Araki K, Maki K, Seki K, Sakamaki K, Harata Y, Sakaino R, et al. Characteristics of a newly developed dentomaxillofacial x-ray cone beam CT scanner (CB MercuRay^{TM}): system configuration and physical properties. Dentomaxillofac Radiol. 2004;33:51–9.
12. Marmulla R, Wörtche R, Mühling J, Hassfeld S. Geometric accuracy of the NewTom 9000 cone beam CT. Dentomaxillofac Radiol. 2005;34:28–31.
13. Arnheiter C, Scarfe WC, Farman AG. Trends in maxillofacial cone-beam computed tomography usage. Oral Radiol. 2006;22:80–5.
14. Bartling SH, Majdani O, Gupta R, Rodt T, Dullin C, Fitzgerald PF, et al. Large scan field, high spatial resolution flat-panel detector based volumetric CT of the whole human skull base and for maxillofacial imaging. Dentomaxillofac Radiol. 2007;36:317–27.
15. Stratemann SA, Huang JC, Maki K, Miller AJ, Hatcher DC. Comparison of cone beam computed tomography imaging with physical measures. Dentomaxillofac Radiol. 2008;37:80–93.
16. Stewart CB. Radiologic science for technologists: physics, biology, and protection. St. Louis: C.V. Mosby; 1988.
17. Samei E, Ranger NT, Dobbins JT III, et al. Intercomparison of methods for image quality characterization. I. Modulation transfer function. Med Phys. 2006;33(5):1454–65.
18. Higashide R, Ichikawa K, Kunimoto H, Sagawa M. Proposal and verification of presampled MTF measurement by the simple analysis method using the edge method (in Japanese). Dent Radiol. 2008;64:417–25.
19. Berland L. Practical CT technology and techniques. New York: Raven Press; 1987.
21. ICRP. ICRP publication 60: 1990 recommendations of the International Commission on Radiological Protection. Annals of the ICRP, vol 21. Oxford: Pergamon Press; 1991.
23. Hayakawa Y, Farman AG, Kelly MS, Kuroyanagi K. Signal-to noise ratio: computed dental radiography versus Sens-A-Ray. Oral Radiol. 1995;11(2):109–13.